

Multi-peak breather stability in a dissipative discrete Nonlinear Schrödinger (NLS) equation

Panayotis Panayotaros* and Felipe Rivero†

*Departamento de Matemáticas y Mecánica,
Instituto de Investigaciones en Matemáticas Aplicadas y en Sistemas,
Universidad Nacional Autónoma de México,
Apdo. Postal 20-726, 01000 México D.F., México*

**panos@mym.iimas.unam.mx*

†feliperivero@mym.iimas.unam.mx

Received 1 September 2014

We study the stability of breather solutions of a dissipative cubic discrete NLS with localized forcing. The breathers are similar to the ones found for the Hamiltonian limit of the system. In the case of linearly stable multi-peak breathers the combination of dissipation and localized forcing also leads to stability, and the apparent damping of internal modes that make the energy around multi-peak breathers nondefinite. This stabilizing effect is however accompanied by overdamping for relatively small values of the dissipation parameter, and the appearance of near-zero stable eigenvalues.

Keywords: Discrete NLS; breathers; dissipative dynamics.

1. Introduction

We study dissipative stabilization effects on multi-peak breather solutions of a discrete NLS equation with spatially dependent forcing. The starting point is the cubic discrete NLS on a finite lattice and nearest-neighbor interaction. This is a Hamiltonian system and has well known periodic solutions of breather-type. In the limit of small intersite coupling these solutions can be spatially localized at arbitrary site configurations.¹ The solutions can also satisfy forced and damped NLS equations provided that the forcing has a spatial dependence that follows the shape of the breather of the Hamiltonian system. These solutions are discrete analogues of the Townes soliton of the continuous forced and damped NLS equation. Recent works on the continuous model use this idea to produce dissipative solitons with more general shapes.^{2,3} The discrete analogue was studied in Ref. 4, where we considered more general solutions.

In this work, the main question is the stability of multi-peak breathers that are linearly stable solutions of the Hamiltonian system. We examine the case of small intersite coupling where the stability of the breather can be understood analytically, following Refs. 5–8. Multi-peak breathers can be linearly stable, but have

both positive and negative energy modes and are not local extrema of the energy (at fixed power). We see that the same solutions remain stable in the forced and damped equation, and it appears that the non-Hamiltonian perturbation suppresses the positive energy modes, leaving a system with an elliptic part with negative definite energy and a dissipative hyperbolic part (positive and negative energy here is specific to the sign conventions we use). Thus forcing and dissipation can provide a mechanism for nonlinear stability, but we also see that some of the internal modes can be easily overdamped, yielding negative eigenvalues that are very near the origin. This suggests that this mechanism is not necessarily very effective in stabilizing breathers with many peaks. Numerical integration with initial conditions near the breather indicate that the attraction to the breather amplitude is efficient for some sites but not for all sites.

The theoretical part of the study is based on the analysis of the Hamiltonian case, and some simple heuristic calculations of the forced and damped problem that are confirmed numerically. It would be an interesting problem to give a mathematical justification of these results. The problem also is an example of a weakly damped system that would be of interest in the theory of dissipative dynamics.

The paper is organized as follows. In Sec. 2, we introduce the forced and damped NLS equation and breather equations. In Sec. 3, we outline the arguments leading to the calculation of the spectra for the forced and damped system. In Sec. 4, we give numerical spectra, and integrate numerically the system to examine the effectiveness of the stabilization mechanism.

2. Dissipative Discrete NLS Equation and Breathers

We consider the dissipative cubic discrete NLS equation

$$\dot{u}_n = i\delta(\Delta u)_n + (2\gamma i - \epsilon)|u_n|^2 u_n + V_n u_n, \tag{2.1}$$

$n \in \{1, \dots, N\}$, where Δ is the discrete Laplacian, defined by

$$(\Delta u)_n = u_{n+1} + u_{n-1} - 2u_n, \quad n = 2, \dots, N - 1, \tag{2.2}$$

$$(\Delta u)_1 = u_2 - 2u_1, \quad (\Delta u)_N = u_{N-1} - 2u_N. \tag{2.3}$$

The particular choice of Δ corresponds to “Dirichlet” boundary conditions (other choices are also possible), and γ, δ are real constants ($\delta\gamma > 0$ is the “focusing” case).

The constant $\epsilon > 0$ describes a nonlinear damping mechanism, while the term $V_n u_n$, with V_n assumed real for all n , represents forcing ($V_n > 0$), or damping ($V_n < 0$) at site n .

The long time behavior of the autonomous dissipative ($\epsilon > 0$) system (2.1) is characterized by its attractor, see Ref. 4. The attractors obtained for different choices of the V_n can be very different and difficult to analyze. In the present work the idea is to study some solutions that appear in the Hamiltonian system obtained from (2.1) by setting $\epsilon = 0, V_n = 0$, for all n , and persist for suitable choices of

the V_n . The NLS system (2.1) with $\epsilon = 0$, $V_n = 0$, for all n , will be referred to as the *Hamiltonian* discrete NLS.

In particular, we study solutions of the discrete NLS (2.1) of the *breather* form $u_n = e^{-i\omega t} A_n$, with ω real, and A_n complex.

By (2.1), A , ω must satisfy

$$-\omega A_n = \delta(\Delta A)_n + (2\gamma - \epsilon)|A_n|^2 A_n + V_n A_n, \quad n \in \{1, \dots, N\}. \quad (2.4)$$

In solving this system one must specify the frequency ω , or some other quantity, see below. Note that if A satisfies (2.4) so does $e^{i\theta} A$, for arbitrary real θ (independent of n). Also a *real* breather is a breather with A_n real, for all n (up to a global phase).

A solution of (2.4) with $\epsilon = 0$, $V_n = 0$, for all n , i.e. a breather solution $u_n = e^{-i\omega t} A_n$ of the Hamiltonian discrete NLS, also satisfies (2.1) and (2.4) with $\epsilon > 0$, provided that

$$V_n = \epsilon |A_n|^2, \quad n \in \{1, \dots, N\}. \quad (2.5)$$

The main question is the stability if these common solutions in the dissipative problem, and the relation of the linear stability analysis of the Hamiltonian and dissipative versions of (2.1) around their common solution. Note that this automatic way of constructing a solution of the dissipative problem from a specific trajectory of the Hamiltonian system by picking a special, generally time-dependent V_n , works for arbitrary trajectories of the Hamiltonian system, see Ref. 4 for pull-back attractors of such systems. Such more general solutions are more difficult to construct.

We briefly review some facts from the analysis of breather solutions of the Hamiltonian problem. Note that (2.1) with $\epsilon = 0$, $V_n = 0$, for all n , can be written in the form of Hamilton's equations

$$\dot{u}_n = -i \frac{\partial H}{\partial u_n^*}, \quad n \in \{1, \dots, N\}, \quad (2.6)$$

with Hamiltonian

$$H = \delta \left(\sum_{n=1}^{N-1} |u_{n+1} - u_n|^2 + |u_1|^2 + |u_N|^2 \right) + \gamma \sum_{n=1}^N |u_n|^4. \quad (2.7)$$

The conserved quantities of system (2.6) are H , and the "power"

$$P = \sum_{n=1}^N |u_n|^2. \quad (2.8)$$

The conservation of P comes from the invariance of H under the (global phase rotation) map $u_n \mapsto e^{i\theta} u_n$, $n \in \{1, \dots, N\}$, with θ arbitrary, independent of n . An analogous equivariance property under global phase rotation is also present in (2.1) for arbitrary ϵ , and forcing V_n .

The existence and calculation of solutions to (2.1) with $\epsilon = 0$, $V_n = 0$, for all n , as been examined by many authors. The first existence proof was given in Ref. 1 for real breathers and $|\delta|$ sufficiently small, i.e. the weak coupling case. This case

is the most amenable to analytical treatment, as the solutions can be obtained as convergent series expansions in the coupling δ . The zeroth-order part is given by the $\delta = 0$ solutions, which can be classified easily as being of the form

$$A_n = \pm \sqrt{-\frac{\omega}{2\gamma}}, \text{ for } n \in U_{\pm}; \quad A_n = 0, \text{ for } n \in U_0, \quad (2.9)$$

with $-\omega\gamma > 0$. The sets U_+ , U_- , U_0 can be arbitrary, and it is assumed that their union is the whole lattice $\{1, \dots, N\}$. If ω is considered fixed, solutions exist only for the right sign of γ . Alternatively one can fix the power P . Such solutions may be termed k -peak breathers, with k the number of sites in the union of U_+ and U_- , i.e. the number of “active” sites.

Note that in the case of $\delta = 0$ each oscillator moves independently, and the general solution of (2.1) consists of oscillations of each site with amplitude dependent frequency, i.e. the breather solutions are very special solutions since the definition forces all nonzero amplitudes to be the same.

As $|\delta|$ is increased the shape begins to change and the sites of U_0 develop non-zero amplitudes. For $|\delta|$ not too large the k -peak description remains accurate, and is mathematically precise as each small $|\delta|$ solution belongs to a solution branch that can be connected (by continuation in δ) to a unique k -peak solution of the $\delta = 0$ problem, see Ref. 7. Generally $\delta \neq 0$ solutions are computed numerically, and there are several theoretical results for higher coupling, generalizations to other types of boundary conditions and lattices, infinite lattices, etc. For instance, all solutions of (2.1) with the particular choice of Δ in (2.2), (2.3) are real,⁹ the same is also the case for decaying breathers in the one-dimensional infinite lattice.¹⁰

The study of the evolution around the breather is simplified by using “moving frame” variables v , defined by $u_n(t) = e^{-i\omega t}v_n(t)$, so that (2.6) is equivalent to

$$\dot{v}_n = -i \frac{\partial H_\omega}{\partial v_n^*}, \quad n \in \{1, \dots, N\}, \quad \text{with } H_\omega = H - \omega P, \quad (2.10)$$

and H as in (2.6). A solution A_n , $n \in \{1, \dots, N\}$, of (2.4) is then a fixed point of (2.10) and belongs to the circle $e^{i\theta}A_n$, $\theta \in \mathbf{R}$, of fixed points of (2.10).

An alternative real notation for (2.10) uses $z = [q, p]^T$, with $z_n = [q_n, p_n]^T$, $q_n = \text{Re } v_n$, $p_n = \text{Im } v_n$, $n \in \{1, \dots, N\}$, i.e. q, p are real vectors. Then (2.10) can be written as

$$\dot{z} = J\nabla h_\omega, \quad \text{with } h_\omega = \frac{1}{2}H_\omega, \quad (2.11)$$

and $(Jz)_n = -[p_n, q_n]^T$, with J the standard symplectic matrix in \mathbf{R}^{2N} .

Using the real notation, the linearization around the breather is

$$\dot{z} = J\mathcal{H}z, \quad \text{with } \mathcal{H} = \nabla^2 h_\omega(A). \quad (2.12)$$

\mathcal{H} is the Hessian of h_ω at A (the dependence of \mathcal{H} on ω is suppressed from the notation). Then (2.12) is equivalent to the Hamiltonian system

$$\dot{z} = J\nabla h, \quad \text{with } h = \frac{1}{2}\langle p, L_+p \rangle + \frac{1}{2}\langle q, L_-q \rangle + \langle q, \tilde{L}p \rangle, \quad (2.13)$$

where L_+ , L_- , \tilde{L} are (real) symmetric $N \times N$ matrices given below. We will consider the simpler case of real breathers, where we see that \tilde{L} vanishes. (This is not a restrictive assumption for the finite problem with the Dirichlet Δ (see Ref. 9)). we study the spectrum of $J\mathcal{H}$, where

$$J = \begin{bmatrix} 0 & I \\ -I & 0 \end{bmatrix}, \quad \mathcal{H} = \begin{bmatrix} L_+ & 0 \\ 0 & L_- \end{bmatrix}, \quad (2.14)$$

$$L_+ = -\omega I - 6\gamma \mathbf{A}^2 - 2\delta\Delta, \quad (2.15)$$

$$L_- = -\omega I - 2\gamma \mathbf{A}^2 - 2\delta\Delta, \quad (2.16)$$

\mathbf{A}^2 is a diagonal matrix with $(\mathbf{A}^2)_{n,n} = A_n^2$, $n = 1, \dots, N$, and I the $N \times N$ identity. The $N \times N$ blocks correspond to the vectors of the real and imaginary components of z , q and p , respectively.

The stability around the breather solution of (2.1) obtained by a breather of the Hamiltonian problem, and the choice of V_n given by (2.5) is studied in the same way, using the moving frame coordinates. The breather is now a fixed point belonging to a circle of fixed points as in the Hamiltonian case, and the linearization around it has the form

$$\dot{z} = (J\mathcal{H} + \epsilon D)z. \quad (2.17)$$

The notation is as in (2.12), and

$$J\mathcal{H} + \epsilon D = \begin{bmatrix} -2\epsilon \mathbf{A}^2 & L_- \\ -L_+ & 0 \end{bmatrix}, \quad (2.18)$$

with L_{\pm} , \mathbf{A}^2 as in the Hamiltonian case.

The above formulation for the linear stability of breathers is valid for arbitrary real breathers. We shall study primarily the case where $|\delta|$ is small. Then there is a rather detailed analysis of the Hamiltonian case, i.e. the matrix $J\mathcal{H}$, and explicit stability criteria that we outline in the next section. These lead to a heuristic study of the dissipative perturbation of $J\mathcal{H}$.

3. Linear Stability of Dissipative Breathers

To study the stability matrix $J\mathcal{H} + \epsilon D$ we consider the small $|\delta|$ regime. We first set $\epsilon = 0$ and summarize some results on the spectrum of $J\mathcal{H}$, following Ref. 7 and ideas from Ref. 5 (see also Ref. 8). We use these results for a simple heuristic analysis of the small ϵ case, assuming *a priori* that $\epsilon \ll |\delta|$. These results are then seen to give a good qualitative prediction of the behavior of the numerically computed spectra of $J\mathcal{H} + \epsilon D$ in the next section.

Note that (2.13) with $\tilde{L} = 0$ describes a linear Hamiltonian system has the mechanical interpretation of a system with “inverse mass matrix” L_+ , and “spring

matrix” L_- , i.e. interpreting q, p as position and momentum coordinates respectively. The matrices L_{\pm} are symmetric but not positive definite, so that the mechanical analogy is not physical. It is instructive however that in the case where L_{\pm} are both diagonal we can read the stability of the system by examining the signs of the eigenvalues. For instance, if entries $(L_+)_{n,n}, (L_-)_{n,n}$ are nonvanishing and have the same sign then h contains the harmonic oscillator part $(1/2)[(L_+)_{n,n}p^2 + (L_-)_{n,n}q^2]$. The oscillator parts lead to pairs of conjugate imaginary eigenvalues for $J\mathcal{H}$. The harmonic oscillator has positive or negative energy, depending on the sign of the $(L_{\pm})_{n,n}$. In the case where $(L_+)_{n,n}, (L_-)_{n,n}$ are nonvanishing and have opposite signs h contains the saddle-node part $\pm(1/2)[|(L_+)_{n,n}|p^2 - |(L_-)_{n,n}|q^2]$, yielding a pair of real eigenvalues of opposite signs for $J\mathcal{H}$, and therefore instability. The case where one of the $(L_{\pm})_{n,n}$ vanishes corresponds to a “free-particle” term $\pm(1/2)[(L_+)_{n,n}p^2]$, or $\pm(1/2)[(L_-)_{n,n}q^2]$ in h , and leads to a pair of zero eigenvalues for $J\mathcal{H}$.

The above considerations are directly applicable to the study of $J\mathcal{H}$ for the $\delta = 0$ breathers in (2.9). Given a k -peak breather solution we see from (2.15), (2.16) that the L_{\pm} are diagonal. For $n \in U_0$ we have $(L_{\pm})_{n,n} = -\omega$, so that h has $N - k$ negative or positive energy harmonic oscillator terms, depending on the sign of ω . (In the next section $\gamma = -1$, so that $\omega > 0$ by (2.9)). These yield $N - k$ pairs of eigenvalues $\pm i\omega$ of $J\mathcal{H}$. For $n \in U_{\pm}$ we have $(L_-)_{n,n} = 0$, and $(L_+)_{n,n} = -4\gamma A^2$, these correspond to free-particle parts in h , and $J\mathcal{H}$ has a zero eigenvalue of multiplicity $2k$. The results are independent of the sets U_{\pm}, U_0 .

For $|\delta| \neq 0$, \mathcal{H} is no longer diagonal, and the eigenvalues move from their $\delta = 0$ positions. The matrices L_{\pm} can not be diagonalized simultaneously and we can not bring the problem to the scenario above. Nevertheless the above considerations are still useful. The spectrum has two main features. First, the eigenvalues $\pm i\omega$ of the $\delta = 0$ matrix spread along the imaginary axis, roughly within the intervals $\pm i[\omega, \omega + 4\delta]$. This fact that can be shown by Krein signature arguments, see also Ref. 7 for the infinite lattice.

The question of stability then rests on the behavior of the zero eigenvalues of the $\delta = 0$ problem, and how they are perturbed for $\delta \neq 0$. It can be shown that there is always a double eigenvalue at the origin, and that the remaining $2k - 2$ eigenvalues are either on the imaginary or the real axis at a distance $O(\sqrt{|\delta|})$ from the origin (for $|\delta|$ small).⁷ The number of real or imaginary eigenvalues of $J\mathcal{H}$ depends on the signs of the perturbed zero eigenvalues of L_- . A simple criterion for $\gamma, \delta > 0$ is in Ref. 5. Since L_- is a symmetric matrix these near-zero eigenvalues can be expressed in powers of δ , and another question is the determination of their leading order term.

We outline one way to calculate the $O(\sqrt{|\delta|})$ eigenvalues of $J\mathcal{H}$. We write the L_{\pm} in block diagonal form

$$L_+ = \begin{bmatrix} A_+ & B_+ \\ C_+ & D_+ \end{bmatrix}, \quad L_- = \begin{bmatrix} A_- & B_- \\ C_- & D_- \end{bmatrix}, \quad (3.1)$$

where the (1, 1) (upper left) block is $k \times k$ and corresponds to the sites in U , the union of U_+ and U_- , i.e. the “active sites” of the $\delta = 0$ problem. The submatrices A_{\pm}, \dots, D_{\pm} are defined by (2.15), (2.16).

Note that the zero eigenvalues of L_- in the case $\delta = 0$ are in A_- . We can diagonalize (approximately) the upper left block of the matrices L_{\pm} by a sequence of (common) similarity transformations by matrices $I + O(\delta^s)$, with increasing $s = 1, \dots, r$. These similarity transformations correspond to linear symplectic changes of coordinates for the variables q, p .

Following this strategy, the L_{\pm} can be transformed after r steps to matrices \tilde{L}_{\pm}^r with blocks

$$A_+^r = \Lambda_1 + O(\delta), \quad B_+^r = O(\delta), \quad C_+^r = O(\delta), \quad D_+^r = \Lambda_2 + O(\delta), \quad (3.2)$$

$$A_-^r = \Lambda_-^r + O(\delta^{r+1}), \quad B_-^r = O(\delta^{r+1}), \quad C_-^r = O(\delta^{r+1}), \quad D_+^r = \Lambda_3 + O(\delta), \quad (3.3)$$

where A_{\pm}^r is $k \times k$, and $\Lambda_1, \Lambda_2, \Lambda_3, \Lambda_-^r$ are diagonal.⁷ The letter-to-block correspondence is as in (3.1).

In Ref. 7 we show that the near-zero eigenvalues of $J\mathcal{H}$ are, to leading order in powers of $\sqrt{\delta}$, eigenvalues of the $2k \times 2k$ matrix $J_k\mathcal{H}_U$ defined by

$$J_k = \begin{bmatrix} 0 & I_k \\ -I_k & 0 \end{bmatrix}, \quad \mathcal{H}_U = \begin{bmatrix} \Lambda_1 & 0 \\ 0 & \Lambda_-^r \end{bmatrix}, \quad (3.4)$$

where I_k is the $k \times k$ identity, $(\Lambda_1)_{n,n} = -4\gamma A^2$ for all n , and (Λ_-^r) has diagonal entries

$$\rho_1 = 0, \quad \rho_2 = c_2\delta^{r_2} + O(\delta^{r_2+1}), \dots, \quad \rho_k = c_k\delta^{r_k} + O(\delta^{r_k+1}), \quad (3.5)$$

with $c_j \neq 0$, and $r_j \leq r$, for all $j = 2, \dots, k$ (i.e. multiple eigenvalues, if any, are repeated). The above statement follows under the assumption that r is sufficiently large and that L_- has only one zero eigenvalue,⁷ other cases are treated similarly. Note that L_- always has a zero eigenvalue, since (2.4), (2.16) imply $L_-A = 0$.

Clearly, (3.4) implies that $J_k\mathcal{H}_U$ has a double zero eigenvalue, and $k - 1$ pairs of eigenvalues

$$\lambda_{k,\pm} = \pm\sqrt{4\gamma A^2\rho_k}, \quad (3.6)$$

i.e. these are real or imaginary depending on the signs of γ , and the ρ_k .

In the case of linear stability of a k -peak breather with $k > 1$, \mathcal{H} can not be definite on the level hypersurfaces of P , and the breather can not be at an extremum of the energy at fixed power. This can be also interpreted in terms of positive and negative energy modes. In the case $\gamma < 0$ (and $\omega > 0$), the $2(N - k)$ negative eigenvalues of \mathcal{H} of the $\delta = 0$ breather, interpreted as $N - k$ negative energy modes of h , remain negative for the small $|\delta|$ breather. On the other hand, the case of linear stability corresponds to the case where \mathcal{H} has $2k$ positive eigenvalues, with k of them of $O(\delta)$, coming from L_- . These positive eigenvalues can be interpreted as positive energy modes.

The theoretical prediction of the eigenvalues of $J\mathcal{H} + \epsilon D$ comes from two assumptions that can not be justified rigorously at present. First we will assume that the imaginary eigenvalues at approximately $\pm i[\omega, \omega + 4\delta]$ remain on the imaginary axis. This can be possibly proved for the infinite lattice problem using the argument of Ref. 7 for $J\mathcal{H}$, but is not clear for the finite lattice case.

The second assumption is that the perturbation of the $O(\sqrt{|\delta|})$ eigenvalues for small $\epsilon > 0$ can be calculated by considering the $2k \times 2k$ matrix $J_k \mathcal{H}_U + \epsilon D_k$, where D_k is the restriction of D to subspaces of the active sites, i.e.

$$J_k \mathcal{H}_U + \epsilon D_k = \begin{bmatrix} -2\epsilon \mathbf{A}_k^2 & \Lambda_k^r \\ -\Lambda_1 & 0 \end{bmatrix}, \tag{3.7}$$

i.e. \mathbf{A}_k^2 is a $k \times k$ diagonal matrix with entries $(\mathbf{A}_k^2)_{n,n} = A^2$ for all $n \in U_+ \cup U_-$. The idea is that A_n is only appreciable for $n \in U_{\pm}$. It can be seen that the steps leading to \tilde{L}_{\pm}^r add terms of $O(\epsilon\delta)$, it is then assumed that these are higher order correction to the eigenvalues computed using (3.7).

The eigenvalues of (3.7) are computed readily for each $n \in U_{\pm}$. We have 2×2 blocks

$$\begin{bmatrix} -2\epsilon A^2 & \rho_n \\ 4\gamma A^2 & 0 \end{bmatrix}. \tag{3.8}$$

In the case of a stable block, i.e. $\gamma\rho_k < 0$, we have the pair of eigenvalues

$$\lambda_{k,\pm} = -\epsilon A^2 \pm \epsilon A^2 \sqrt{1 - \frac{4|\gamma\rho_k|}{\epsilon^2 A^2}}. \tag{3.9}$$

For $\epsilon > 0$ and sufficiently small the $\lambda_{k,\pm}$ are both complex and have negative real part $-\epsilon^2 A^2$. For

$$\epsilon^2 \geq \frac{4|\gamma\rho_k|}{A^2}, \tag{3.10}$$

both eigenvalues are real, and negative, we thus have overdamping. As $\epsilon \rightarrow \infty$ we have $\lambda_{k,-} \rightarrow -\infty$, $\lambda_{k,+} \rightarrow 0$. For large ϵ we therefore have a negative eigenvalue that is close to the origin. In fact, for $A, \gamma \sim 1$ the overdamping condition is already satisfied for very small $\epsilon \sim 2\sqrt{\rho_k}$, i.e. comparable to the modulus of the corresponding eigenvalue of $J\mathcal{H}$.

In the case of an unstable block, i.e. $\gamma\rho_k > 0$, we have the pair of eigenvalues

$$\lambda_{k,\pm} = -\epsilon A^2 \pm \epsilon A^2 \sqrt{1 + \frac{4|\gamma\rho_k|}{\epsilon^2 A^2}}. \tag{3.11}$$

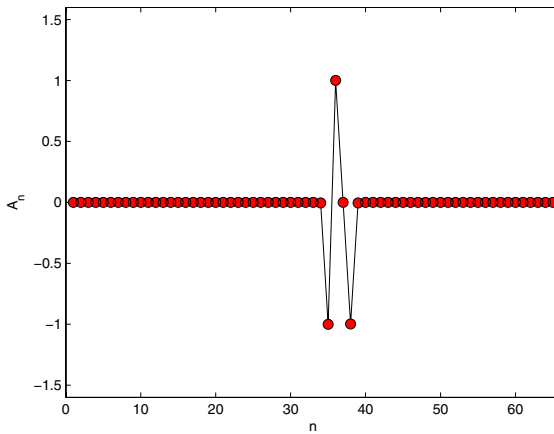
Both eigenvalues are real, with $\lambda_{k,-}$ negative, and $\lambda_{k,+}$ positive, for all $\epsilon > 0$. We thus always have instability. As $\epsilon \rightarrow \infty$ we have $\lambda_{k,-} \rightarrow -\infty$, and $\lambda_{k,+} \rightarrow 0$, i.e. the instability becomes weaker.

4. Numerical Results for Stable Breathers of the Dissipative NLS

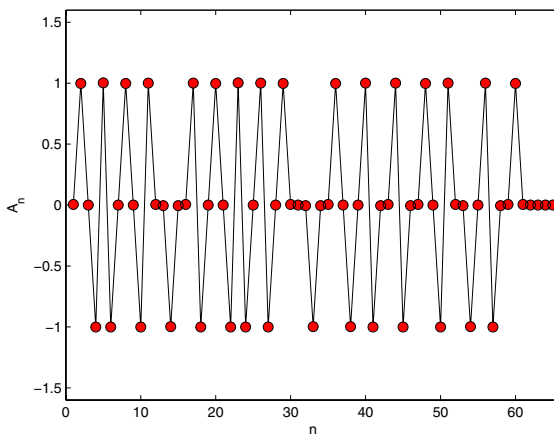
In this section, we give some numerical results on the stability of different breathers, focusing on breathers that are linearly stable in the Hamiltonian case. We verify numerically the qualitative picture of the previous section for the stability of forced and damped breather solutions. We also integrate numerically the equations of motion. We see that the stabilizing effect of the forcing and dissipative terms drives the amplitude of many, but not all, sites closer to the breather amplitude.

In what follows we consider (2.1) with $\gamma = -1$, and the corresponding breather solutions.

We first consider the spectrum around breathers that are linearly stable in the Hamiltonian system. Figures 1(a) and 1(b) show examples with 3-, and 31-peak



(a)



(b)

Fig. 1. (a) Amplitudes A_n of 3-peak real breather. (b) Amplitudes A_n of 31-peak real breather. In both cases the sign of A_n at the peak sites alternates. $N = 65$, $\delta = -0.01$, $\gamma = -1.0$.

profiles, respectively. We use $N = 65$ sites, and $\delta = -0.01$ (focusing case). The power is chosen proportional to the number of peaks so that the amplitude is near unity at the active sites, while $\omega \sim 2$. In both cases the breather amplitudes have alternating signs at the active sites, and this leads to linear stability under the Hamiltonian evolution.⁵

The number of $O(\delta)$ eigenvalues in L_- is $k-1$ for the k -peak soliton as expected, and this leads to the $k-1$ pairs of conjugate imaginary eigenvalues. These are easily distinguished from the eigenvalues near $\pm i\omega \sim \pm 2i$ in these examples.

In Fig. 2, we examine the linear stability of the 3-peak example of Fig. 1(a), plotting the spectra, as we vary ϵ from 0 to 0.2. The near-zero eigenvalues of the $\epsilon = 0$ case are $\pm i0.0173313673$, $\pm i0.283961297$, and Fig. 2 indicates that one of the pairs, the one starting nearest to zero is already overdamped at $\epsilon = 0.2$. The other pair still has nonvanishing imaginary part at $\epsilon = 0.2$. The dependence of the eigenvalues on ϵ before overdamping has the parabolic shape suggested by (3.11). We verify that overdamping of the eigenvalue starting from $\pm i\rho_k$ starts at about $\epsilon = \rho_k$, as in (3.10) with $|A| \sim |\gamma| = 1$.

The window used in Fig. 1(a) does not include the eigenvalues that start near $\pm i\omega$ at $\epsilon = 0$, these have positive and negative real parts that are at most 10^{-7} for all $\epsilon \in [0, 0.2]$. These real parts are near the numerical accuracy of the eigenvalue calculations here, and we can not determine whether the eigenvalues leave the imaginary axis.

In the 31-peak example of Fig. 1(b) we have many more eigenvalues that are smaller than $O(\sqrt{\delta})$ in the Hamiltonian problem, e.g. eigenvalues $\pm i2.5 \times 10^{-5}$, $\pm i3.5 \times 10^{-4}$, $\pm i3.6 \times 10^{-4}$, $\pm i7.5 \times 10^{-4}$, etc. In Fig. 3(a) we show the spectra varying ϵ from 0 to 0.15. We see that all but a few eigenvalues are overdamped. The eigenvalues that are not overdamped shown in the figure start at approximately

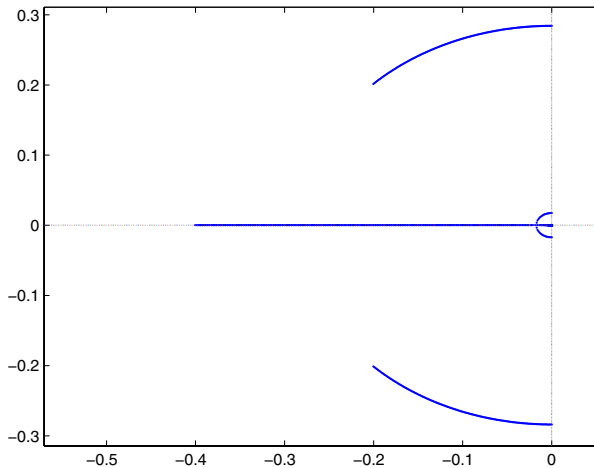
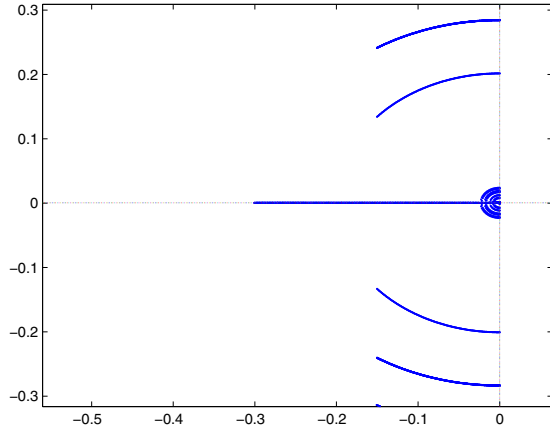
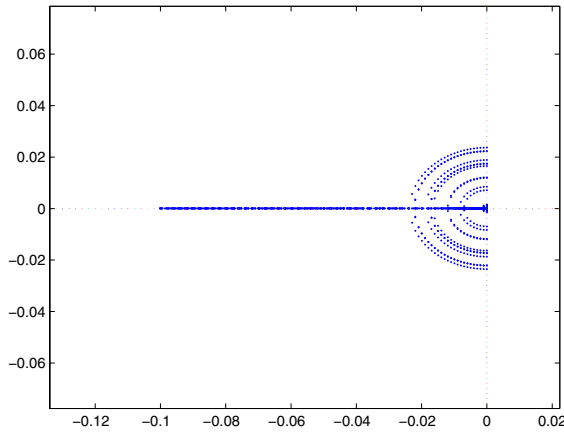


Fig. 2. Eigenvalues of $J\mathcal{H} + \epsilon D$ for 3-peak breather of Fig. 1(a) as we vary ϵ from 0 to 0.2 (step 0.001).



(a)



(b)

Fig. 3. (a) Eigenvalues of $J\mathcal{H} + \epsilon D$ for 31-peak breather of Fig. 1(b), ϵ is varied from 0 to 0.15 (step 0.001). (b) Zoom of (a) near the origin, ϵ varies from 0 to 0.05.

$\pm i0.28$, $\pm i0.2$ at $\epsilon = 0$. There are more than the two pairs suggested by the two branches shown, but are too close to be distinguished in the picture. In Fig. 3(b) we vary ϵ from 0 to 0.05 and zoom at the eigenvalues that are near the origin. These are all overdamped at $\epsilon = 0.05$. Figures 3(a) and 3(b) do not include the eigenvalues that start near $\pm i\omega$ at $\epsilon = 0$, the remarks for the 3-peak example apply here as well.

The above confirm the picture suggested by the heuristic analysis of the previous chapter. The $O(\sqrt{\delta})$ eigenvalues of $J\mathcal{H}$ become stable, while the other eigenvalues remain on, or in the vicinity of the imaginary axis. Similar results were seen in more examples.

Numerical integration of initial conditions near the stable breathers above and some other examples shows that the amplitude profiles change little for both the Hamiltonian and forced and damped cases. We integrate up to $t = 400$, with $\epsilon = 0$, 0.001, and 0.10. The perturbation is of the order of 10^{-2} . In the Hamiltonian case $\epsilon = 0$ we see the amplitude profile stays close to the initial one, with possible slow oscillatory growth at some inactive sites. Nevertheless the amplitude of all sites remains to $O(10^{-2})$ of the initial amplitude, and this is also seen for up to $t = 800$. We do not see therefore at this time scale any significant departure from the predictions of the linearization. In the cases of positive ϵ we see that the amplitude of some nodes approaches their value for the breather solutions. This is not however true for all sites, where we see that the difference from the breather amplitude remains close to the initial one. This may be related to the presence of overdamping and the resulting stable eigenvalues that are too near the origin in both examples.

5. Discussion

We have studied breathers of a dissipative discrete NLS equation with localized forcing. The combination of dissipation and localized forcing that matches the pattern of breather solutions of the Hamiltonian discrete NLS seems sufficient to damp the positive energy internal modes present in multi-peak breathers of the Hamiltonian system. This leads to the possibility that linearly stable multi-peak solutions of the Hamiltonian limit become asymptotically stable in the infinite lattice.

At the same time we see that the internal modes can be overdamped even for small values of the dissipation parameter. Overdamping leads to stable eigenvalues that are very near the origin, and this limits the strength of this stabilization mechanism. For the relatively small perturbations of the breather and timescales studied numerically here, the Hamiltonian and dissipative problems look quite similar. Trajectories do not leave the vicinity of the breather, and the addition of dissipation leads to some damping of the perturbation, at some but not all the sites. Further studies will be needed to examine larger perturbations from the breather in the Hamiltonian and dissipative cases.

The heuristic study of the stability of the dissipative breathers also includes the case of linearly unstable breathers of the Hamiltonian problem. These are expected to remain linearly unstable in the dissipative case, but with vanishing positive eigenvalues in the strongly damped case. The dynamics of these cases may be more interesting and could be investigated in further work.

Acknowledgments

P. Panayotaros acknowledges partial support from SEP-Conacyt grant 177246, and FENOMECE. F. Rivero acknowledges partial support from MEC grant MTM 2011-22411.

References

1. R. S. MacKay and S. Aubry, Proof of existence of breathers for time-reversible or Hamiltonian networks of weakly coupled oscillators, *Nonlinearity* **7** (1994) 1623–1643.
2. C. K. Lam, B. A. Malomed, K. W. Chow and P. K. A. Wai, Spatial solitons supported by localized gain in nonlinear optical waveguides, *Eur. Phys. J. Special Topics* **173** (2009) 233–243.
3. Y. V. Kartashov, V. V. Konotop and V. A. Vysloukh, Two-dimensional dissipative solitons supported by localized gain, *Opt. Lett.* **36** (2011) 82–84.
4. P. Panayotaros and F. Rivero, Multistability and localization in a dissipative discrete NLS equation, *Disc. Cont. Dyn. Syst. B* **19** (2014) 1137–1154.
5. D. E. Pelinovsky, P. G. Kevrekidis and D. J. Frantzeskakis, Stability of discrete solitons in nonlinear Schrödinger lattices, *Phys. D* **212** (2005) 1–19.
6. D. E. Pelinovsky, P. G. Kevrekidis and D. J. Frantzeskakis, Persistence and stability of discrete vortices in nonlinear Schrödinger lattices, *Physica D* **212** (2005) 20–53.
7. P. Panayotaros, Linear stability of breathers of the discrete NLS, *Phys. Lett. A* **373** (2009) 957–963.
8. D. Pelinovsky and A. Sakovich, Internal modes of discrete solitons near the anti-continuum limit of the dNLS equation, *Physica D* **240** (2011) 265–281.
9. P. Panayotaros, Continuation and bifurcation of breathers in a finite discrete NLS equation, *Disc. Cont. Dyn. Syst. S* **4**, **5** (2011) 1227–1245.
10. W. Qin and X. Xiao, Homoclinic orbits and localized solutions in nonlinear Schrödinger lattices, *Nonlinearity* **20** (2007) 2305–2317.